Supplemental Information

Supplemental Figures

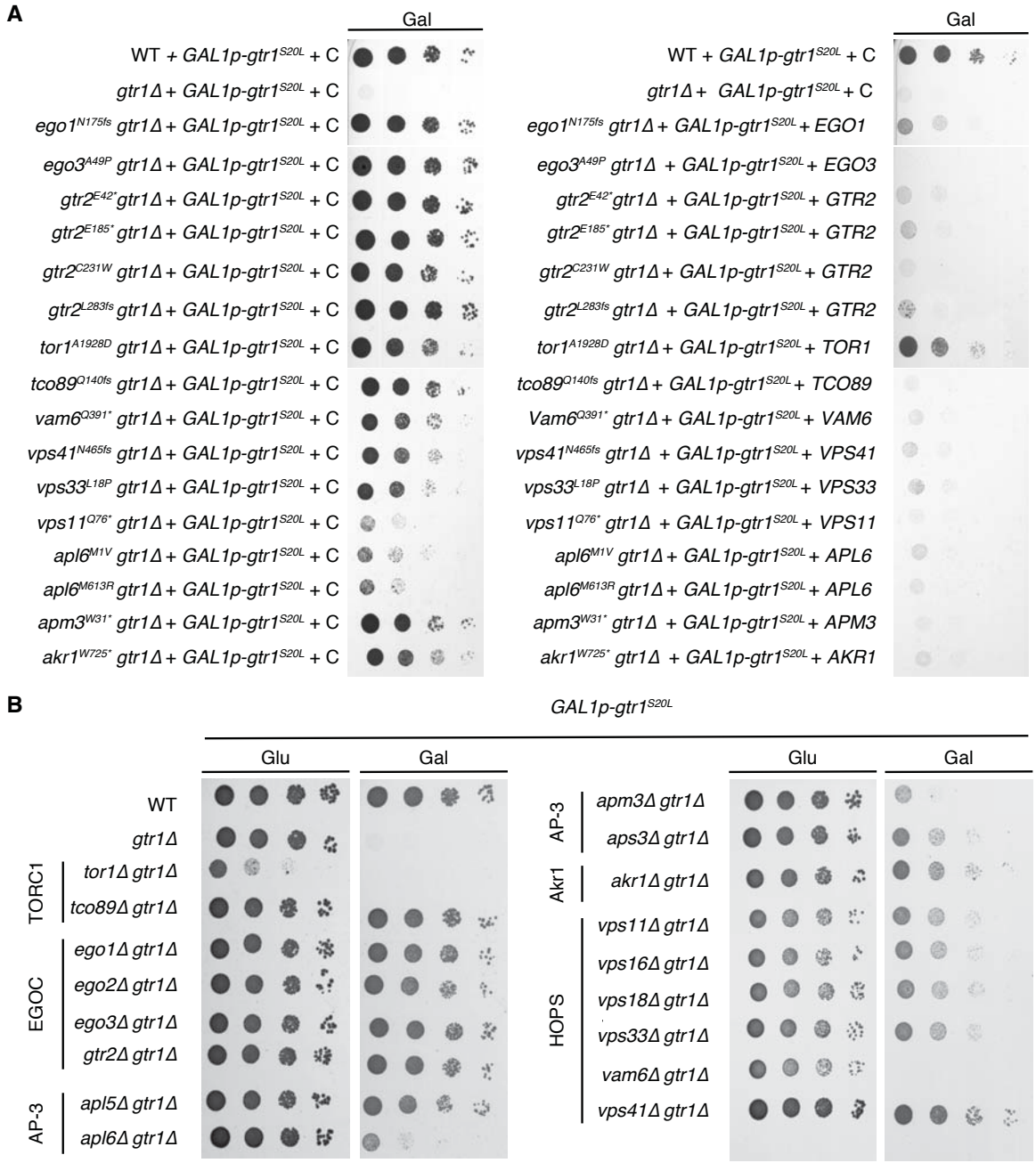

Figure S1. Analysis of Suppressors of the Gtr1^{S20L}-Mediated Growth Inhibition, Related to Table 1

(A) Complementation analysis of the mutations (see Table 1) that suppress the Gtr1^{S20L}-mediated growth inhibition. The ability of the indicated double mutants to grow when Gtr1^{S20L} was overproduced from the galactose-inducible *GAL1* promoter was analyzed in the absence (empty plasmid control; + C) and presence (+ *GENE*) of the respective indicated (plasmid-expressed) wild-type genes after cells were spotted (10-fold serial dilutions) and grown for 3 days at 30°C on galactose (Gal).

(B) To independently confirm the results from our selection for mutations that suppress the growth inhibition of overproduced Gtr1^{S20L}, the respective genes were deleted in a *gtr1*Δ background. Strains were analyzed as in (A).

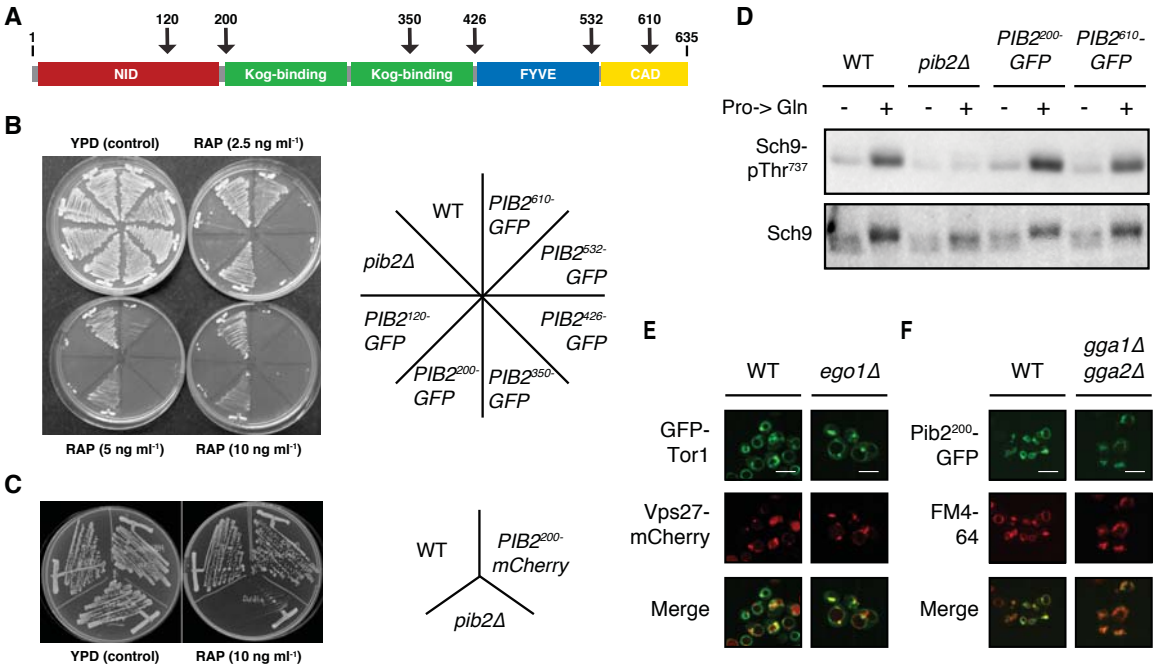

Figure S2. Construction of a Functional Pib2^{200}-GFP, Related to Figures 2J-L

(A) Schematic depiction of GFP integration sites in Pib2. The positions for the integration of GFP were chosen so that they would not interfere with the FYVE domain, the C-terminal tail motif, or with any region with a potential secondary structure according to Jpred 4 (http://www.compbio.dundee.ac.uk/jpred/). For further details, see also (Kim and Cunningham, 2015; Michel et al., 2017). Of note, our attempt to fuse GFP at either N- or C-terminus of Pib2 ended up with impairing its function (data not shown).

(B, C) Strains expressing genomically-tagged Pib2^{200}-GFP (B) and Pib2^{200}-mCherry (C) are fully functional, while Pib2^{610}-GFP is partially functional with respect to rapamycin sensitivity. Indicated strains were streaked and grown for 3 days on YPD plates containing, or not (control), indicated concentrations of rapamycin.

(D) Pib2^{200}-GFP and Pib2^{610}-GFP normally mediate TORC1 activation by glutamine. Indicated strains were grown to mid-log phase in SD-proline medium (-) and stimulated with 3 mM glutamine for 2 minutes (+). TORC1 activity was assessed as in Figure 3C.

(E, F) GFP-Tor1 colocalizes with Vps27-mCherry in WT and *ego1*Δ cells (E), and Pib2^{200}-GFP colocalizes with FM4-64 in WT and *gga1*Δ *gga2*Δ cells, but only assembles on endosomes in WT cells (F). See also Figure 2. Scale bars, 5 µm (white).

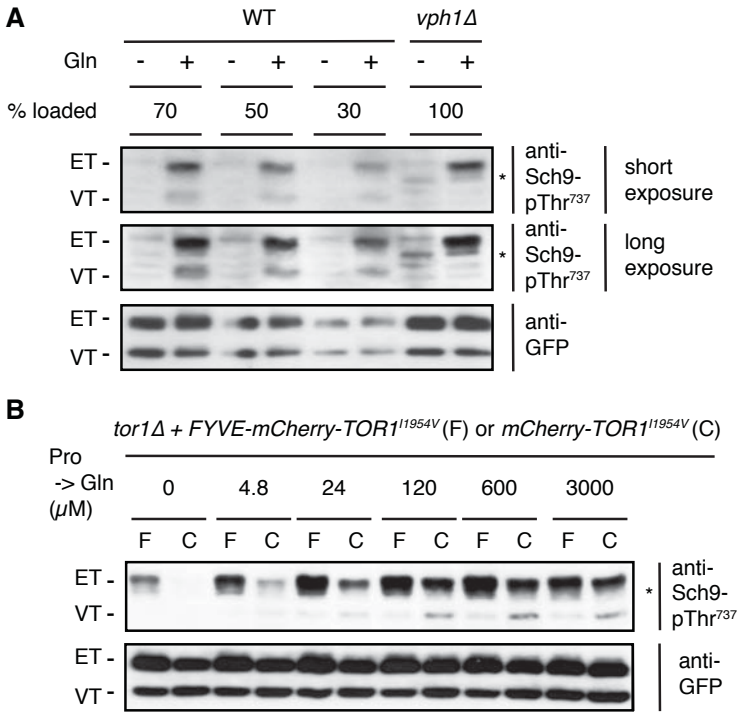

Figure S3. Vph1 is Essential to Ensure Vacuolar TORC1 Activity and Artificial Tethering of mCherry-Tor1^{I1954V} to Endosomes Depletes Vacuolar TORC1 Activity, Related to Figures 4A and 4E

(A) Loss of Vph1 abolishes the glutamine-stimulated phosphorylation of the vacuolar TORC1 reporter, but only mildly affects the respective phosphorylation of the endosomal TORC1 reporter. Indicated dilutions of the WT sample were compared to 100% of the *vph1*Δ sample (both from Figure 4A), this latter serving as a reference of endosomal reporter (ET) phosphorylation in response to 3 mM glutamine stimulation. Similar signal intensity was obtained with 70% of the WT sample (compare ET phosphorylation in lanes 2 and 8), indicating that loss of Vph1 slightly compromises endosomal TORC1. Remarkably, in these same samples, phosphorylation of the vacuolar reporter (VT) was not detected in *vph1*Δ even after prolonged exposure of the immunoblots (compare VT phosphorylation in lanes 2 and 8), indicating that Vph1 is specifically required for glutamine-triggered vacuolar TORC1 activation.

(B) mCherry-Tor1^{I1954V} mediates phosphorylation of both endosomal and vacuolar TORC1 reporters, while its artificial hooking to endosomes (through a fusion with a FYVE domain) specifically impairs its ability to phosphorylate the vacuolar reporter in glutamine-stimulated cells. *tor1*Δ cells expressing mCherry-Tor1^{I1954V} (Control; C) or FYVE-mCherry-Tor1^{I1954V} (FYVE; F) were grown as in Figure 4E, and stimulated with increasing concentrations of glutamine for 2 min. Upon stimulation with 3 mM glutamine, both constructs similarly triggered maximal phosphorylation of the endosomal reporter (ET), while endosome-targeted FYVE-mCherry-Tor1^{I1954V} failed to phosphorylate the vacuolar reporter (VT). Of note, only FYVE-mCherry-Tor1^{I1954V} sustained, as expected, ET phosphorylation after stimulation (or not) with very low levels of glutamine (*i.e.* < 5 µM).

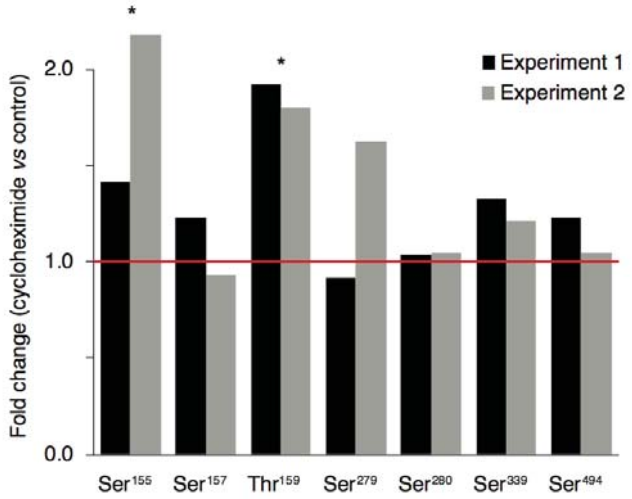

Figure S4. SILAC-Based Quantification of TORC1-Responsive Vps27 Phosphosites *In Vivo*, Related to Figure 5C

Bar diagram lists the phosphosites identified on purified Vps27 comparing SILAC labeled cycloheximide treated to untreated control cells. *: sites identified as increased by a minimum of 80% (average value, n = 2).

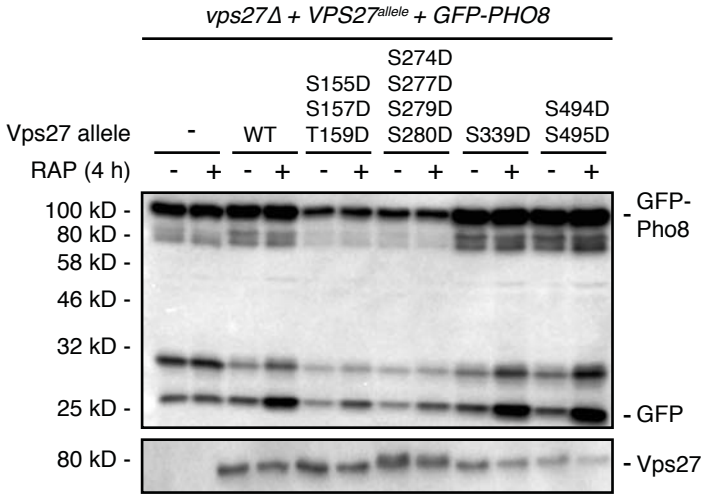

Figure S5. TORC1 Impinges on Vps27 to Inhibit ESCRT-Driven Degradation of Vacuolar Membrane-Resident GFP-Pho8, Related to Figure 5F

Cells expressing, or not (-), indicated Vps27 alleles from plasmids were grown exponentially (-) and then treated with rapamycin (200 ng ml^{-1}; +) for 4 hours. Corresponding cell extracts were subjected to immunoblot analyses using anti-GFP antibodies to measure the levels of GFP-cleavage from plasmid-expressed GFP-Pho8. The levels of Vps27 variants were analyzed by immunoblot analysis using anti-Vps27 antibodies.

Supplemental Table

Table S1. TORC1-Controlled Phosphorylation Sites in Vps27[a], Related to Figure 5A

Peptide	Positions	PEP	Score	Phospho-Ser/Thr Probabilities
P1-Vps27-Sc	159	5.2E-110	115	LTLS(0.008)NS(0.024)PT(0.966)AMFDS(0.002)K
P2-Vps27-Sc	274	0.0014	62	AIELS(0.01)LKES(0.99)R
P3-Vps27-Sc	279	5.8E-56	88	NS(0.013)AS(0.929)S(0.058)EPIVPVVESK
P3-Vps27-Sc	280	8.6E-23	69	NS(0.001)AS(0.088)S(0.911)EPIVPVVESK
P1-Vps27-Ec	155	1.38E-10	117	LTLS(0.994)NS(0.006)PTAMFDSK
P1-Vps27-Ec	157	< 4.0E-128	362	LTLSNS(1)PTAMFDSK
P2-Vps27-Ec	274	0.0007	125	AIELSLKES(1)R
P3-Vps27-Ec	277	1.3E-38	165	NS(1)ASSEPIVPVVESK
P3-Vps27-Ec	280	4.0E-128	218	NSASS(1)EPIVPVVESK
P4-Vps27-Ec	339	1.1E-08	72	QMQPQQPS(1)PQPQPIHSVDLSDEEK
P5-Vps27-Ec	495	8.9E-37	161	ANS(0.003)S(0.997)PTTNIDHLK

[a]Vps27 isolated from *S. cerevisiae* (Vps27-Sc) or codon-optimized Vps27 (coexpressed with Hse1) isolated from *E. coli* (Vps27-Ec) were phosphorylated by TORC1 *in vitro*. Subsequent MS-analysis allowed the identification of the same 3 phosphopeptides (P1-3) in Vps27-Sc (green shading) and in Vps27-Ec (blue shading) and two additional ones in Vps27-Ec (P4/5; blue shading). The phospho-Ser/Thr localization probabilities indicate the positions of the most likely phosphorylated amino acid residues. Sites marked in blue and the ones marked in yellow (*i.e.* Thr^{159} and Ser^{279} that were identified as potential TORC1 target sites in Vps27-Sc [phospho-Ser/Thr probability > 0.9]) were exchanged to alanines to create the $Vps27^{10A}$ for the *in vitro* TORC1 kinase assay in Figure 5B. The sites marked in red were exchanged to phospho-mimetic aspartates to create $Vps27^{7D}$ for *in vivo* studies in yeast. PEP: posterior error probability; Score: Andromeda score.